Applied Physics Letters

Carrier transport and confinement in polarization-induced three-dimensional electron slabs: Importance of alloy scattering in AlGaN

Cite as: Appl. Phys. Lett. **88**, 042109 (2006); https://doi.org/10.1063/1.2168253
Submitted: 03 August 2005 . Accepted: 01 December 2005 . Published Online: 26 January 2006

John Simon, Albert (Kejia) Wang, Huili Xing, Siddharth Rajan, and Debdeep Jena

Carrier transport and confinement in polarization-induced three-dimensional electron slabs: Importance of alloy scattering in AlGaN

John Simon, Albert (Kejia) Wang, and Huili Xing
Department of Electrical Engineering, University of Notre Dame, Notre Dame, Indiana 46556

Siddharth Rajan
Department of Electrical and Computer Engineering, University of California at Santa Barbara, Santa Barbara, California 93106

Debdeep Jena[a)]
Department of Electrical Engineering, University of Notre Dame, Notre Dame, Indiana 46556

(Received 3 August 2005; accepted 1 December 2005; published online 26 January 2006)

By exploiting the difference in spontaneous and piezoelectric polarization between GaN and compositionally graded layers of strained AlGaN, we demonstrate three-dimensional electron slabs of tunable widths (30–100 nm) and densities ($1–5\times10^{18}$ cm^3). Removal of ionized impurity scattering results in relatively high mobilities limited by alloy scattering at low temperatures, and by a combination of alloy and polar optical phonon scattering at room temperature. Owing to the tunable electron-electron interactions in such slabs, they offer an ideal system to probe high-field transport physics in the III-V nitride semiconductors in general, and the hot-phonon effect in particular. © *2006 American Institute of Physics*. [DOI: 10.1063/1.2168253]

Recently, there has been a lot of interest in high-field electron transport in wide-band-gap semiconductors, especially for the highly polar III-V nitrides. One of the motivations is to make field-effect transistors that operate in the mm-wave regime (30–300 GHz). Recent reports[1,2] indicate that there may be a hot-phonon bottleneck in III-V nitride high-electron mobility transistors that reduces the velocity of carriers in very high electron-density channels [typical two-dimensional (2D) electron gas (2DEG) densities are $n_{2D}\sim10^{13}$ cm^2]. The bottleneck arises from the fast emission ($\sim$10 fs) of a large number of polar optical phonons, which decay slowly ($\sim$1–5 ps).[3] It is believed that the buildup of nonequilibrium polar optical phonons adversely affects the speed of devices. A proposed solution[1,4] is to: (a) Lower the effective volume density of carriers, thereby reducing the strength of electron-electron (e-e) interactions, and at the same time, (b) maintain a high channel conductivity that the 2DEG enjoys due to the high sheet density and high mobility due to lack of impurity scattering. In this work, we present a scheme that achieves these two goals; the high-field transport analysis is the subject of a later work.

Wurtzite III-V nitrides exhibit large polarization fields[5] that are not present in other material systems. It has been shown earlier[6] that these fields can be engineered at abrupt, as well as compositionally graded heterojunctions to produce regions of high mobility 2D and three-dimensional (3D) electron slabs (3DES). These polarization-induced electron channels are resistant to carrier freezeout at low temperatures, and also exhibit high mobilities compared to impurity doped structures. In this work, the continuous tuning of carrier volume density, its confinement, and the scattering processes that dominate transport properties of such electron gases in III-V nitride alloys are presented.

Figure 1 shows the sample structures and the calculated band diagrams and charge distributions for the studied AlGaN/GaN samples. The samples were grown by metalorganic vapor deposition and the aluminum composition was graded linearly from $x=0\rightarrow x=30\%$ over different thicknesses, d. Three samples with graded layer thickness of $d=30$, 50, and 100 nm were studied. Ohmic contacts were defined by annealed Ti/Al/Ni/Au metal stacks, and Ni/Au stacks were used for Schottky gates. Polarization-induced bulk doping of different densities results from the compositional grading of aluminum composition; the dependence follows $\rho_\pi\sim\Delta P(x)/d$, as described earlier.[6,7] Spontaneous and piezoelectric polarization differences between the AlGaN and GaN layers $\Delta P(x)$ create positive polarization charges in the graded layer region. The band diagrams and charge distributions calculated by a self-consistent Schrodinger–

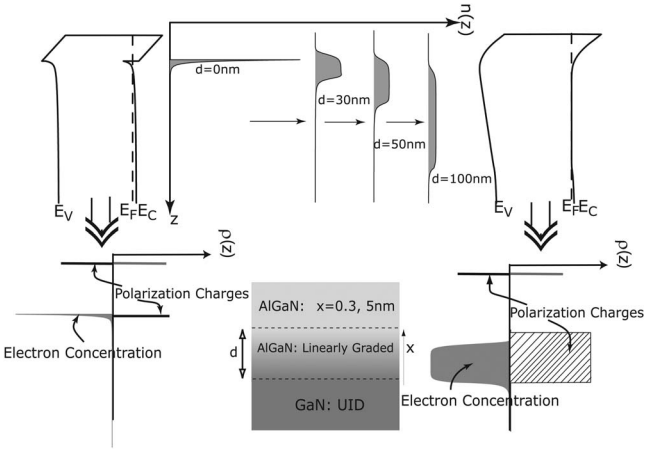

FIG. 1. Sample structures and calculated self-consistent band diagrams and charge distributions. The mobile electron concentration $n(z)$ decreases with increasing graded layer thickness d, though the sheet density remains constant.

[a)]Electronic mail: djena@nd.edu

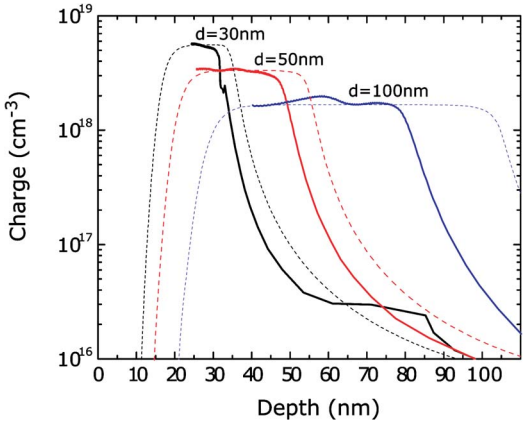

FIG. 2. (Color online) Room-temperature capacitance-voltage measurements performed on three linearly graded AlGaN/GaN layers. Solid lines represent the apparent carrier profile obtained from the experimental data and dashed lines represent simulated data.

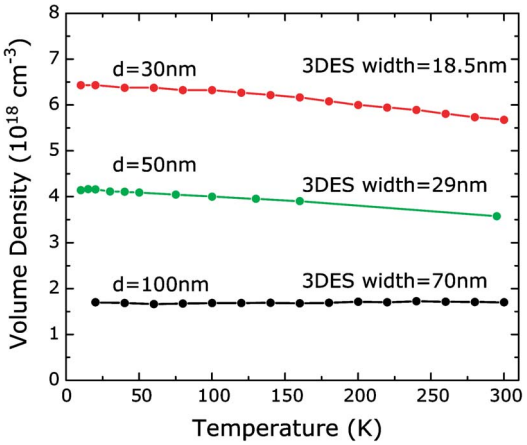

FIG. 3. (Color online) 3DES density dependence on temperature from Hall measurement for the three polarization-doped layers.

Poisson solution in the effective mass approximation for the structures is shown in Fig. 1, illustrating the gradual tuning from a 2D to 3D electron population.

The gate capacitance as a function of voltage was measured for all three samples, and carrier profile as a function of position was extracted. Figure 2 shows the measured and calculated carrier profile for the three samples. In all three samples, the mobile carrier density is seen to be confined within the graded layer region. The volume carrier density is seen to change from $\sim 5\times 10^{18}$ cm^{-3} to $\sim 1.6\times 10^{18}$ cm^{-3} when the graded layer thickness is varied from 30 nm to 100 nm. This demonstrates the flexibility of polarization-induced doping—one can change the material composition (demonstrated earlier)[6] and/or the graded layer thickness to produce the desired carrier density. The homogeneous model used to determine the electron concentration results in a mismatch between the theoretical and experimental carrier profiles; a heterojunction model will lead to better accuracy.[8] It is important to note that the thermal de-Broglie length of electrons in GaN at room temperature is $\lambda_{dB}=2\pi\hbar/\sqrt{2m^{\star}kT}=17$ nm, indicating that the confinement of the 3DES is indeed weak in the growth direction.

By assuming a Fang–Howard variational wave function approximation,[9] it is straightforward to show that the "thickness" of a 2DEG (approximated here by the full width at half maximum of the density distribution) is given by $\sim 3.4/b$, where $b=(33m^{\star}e^2n_{2D}/8\hbar^2\epsilon)^{1/3}$ is the variational parameter that depends on the 2DEG sheet density. Here, $m^{\star}$ is the conduction-band electron effective mass, e is the electron charge, $\hbar$ is the reduced Planck's constant, and ϵ is the dielectric constant. Using this for a nominal AlGaN/GaN abrupt heterojunction, a 2DEG of effective sheet density 10^{13} cm^2 has a nominal thickness of only 2.6 nm. For the same total difference in polarization between AlGaN and GaN, one obtains the same *sheet* density in a 3DES; however, for the 3DES, the thickness is indeed *tunable* over a wide range (30–100 nm shown in this work). For comparing the e-e interaction strength, we use the widely used metric r_s.[10] For 3DES densities ranging from 10^{17}–10^{19} cm^3, r_s ranges from 5.7–1.2. The same parameter for a 2DEG of density 10^{13} cm^2 is $r_s=0.83$, implying very strong e-e interaction. Thus, by exploiting the large polarization fields in the III-V nitrides, the 3DES offers an attractive route to lower the strength of e-e interactions.

Temperature dependent Hall measurements were performed on van der Pauw patterns defined on the three samples. These measurements were performed by placing the samples in a helium closed-cycle refrigerator and varying the temperature from 10 K to 300 K with a resistive heater at low magnetic fields (<1 T). Figure 3 shows the 3DES carrier density, and Fig. 4 shows the measured mobility over a wide temperature range. The polarization-induced 3DES density is remarkably resistant to temperature changes. The Hall mobility is seen to vary from ~ 900 cm^2 V s at room temperature to ~ 3000 cm^2 V s at 10 K. The advantages emanating from the high conductivity of such electron gases over impurity-doped electron channels for device applications are outlined in an earlier work.[6] Here, we concentrate on identifying the scattering mechanisms that determine the carrier transport properties. Figure 4 also includes the theoretically calculated contributions of individual scattering mechanisms and the calculated total mobility; the theoretical values seem to explain the experimental numbers reasonably well.

We include scattering processes from polar optical phonons (Ref. 11) $\hbar\omega_0=92$ meV (GaN) and 100 meV (AlN), acoustic phonons due to deformation potential and piezoelectric interactions, ionized impurity scattering ($N_{imp}=10^{17}$ cm^3), charged dislocation scattering[12–14] ($N_{disl}=10^9$ cm^2), and alloy disorder scattering[15] in our calculation. In order to model the measured mobility theoretically, we assume a constant volume density of the 3D electrons (this is approximately true for all three samples, as seen in Fig. 3). The Fermi energy is then determined as a function of temperature from the Joyce–Dixon approximation.[16] This enables us to use exact ensemble-averaged forms for the scattering rates for each scattering process considered. Appropriate Hall factors are used to convert the drift mobility to Hall mobility, and the scattering rates are evaluated for the whole graded layer, taking into account the spatially varying dielectric constant, alloy composition, and optical-phonon energy. The size of the unit cell is assumed to be the same as that of unstrained GaN, since the AlGaN layers are coherently strained. The total mobility is then calculated by a Matheissen's rule sum of the individual components.

Coulombic scattering processes arising from ionized impurities and charged dislocations are found to be weak (compared to alloy disorder and phonon scattering) due to heavy screening. In fact (from Fig. 4), the whole temperature de-

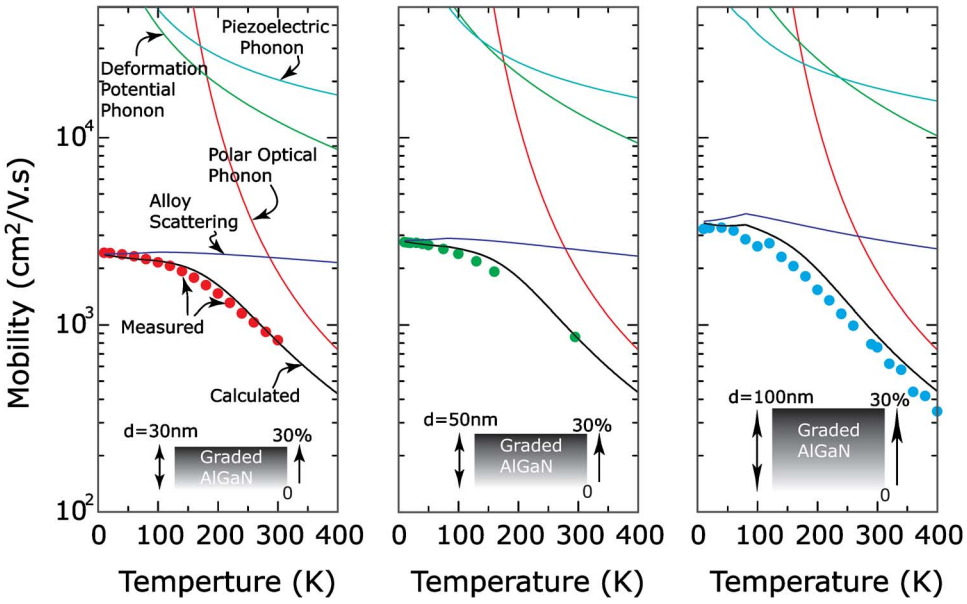

FIG. 4. (Color online) Measured and calculated mobilities vs temperature for three graded AlGaN layers with the 3DES spread over 30, 50, and 100 nm. The various scattering mechanisms included show that room-temperature mobility is limited by a combination of optical phonon and alloy scattering, whereas alloy scattering dominates at low temperatures for all three samples.

pendence of mobility may be explained by considering two scattering processes only—alloy disorder and polar optical phonons. Alloy scattering is identified as the dominant scattering mechanism at low temperatures, and is rather strong even at high temperatures. A short-range alloy scattering potential (Ref. 15) $V_0=1.5$ eV is found to explain the mobility variation of all three samples, which is smaller than the conduction-band discontinuity of $\Delta E_C=2.1$ eV between GaN and AlN. The fact that alloy scattering in the 3DES is dominant at low temperatures supports recent reports[17] of intrinsic mobility limits in AlGaN/GaN 2DEGs as well.

Thus, the mobility obtained might be close to the intrinsic limits set by the statistical disorder in the alloy system. If this is true, the low-field conductivity of such layers may be further improved upon by switching to a "digital" $(AlN)_n$-GaN_m superlattice alloy growth scheme[18] which removes the spatial disorder in the alloy composition. However, the inplane electron transport properties of such digital alloy layers have not been looked into for III-V nitrides to date.

In summary, we have demonstrated the use of polarization fields in III-V nitrides to produce high-conductivity 3DES with tunable carrier densities and confinement without impurity doping. These slabs have higher mobilities compared to impurity doped structures of similar densities. We verify the two degrees of freedom available to establish the desired polarization-induced doping density, and we observe no carrier freeze out at low temperatures. Fits done to measured mobility show a clear dominance of alloy and phonon scattering at low fields. The 3DES demonstrated here provide an ideal test bed for clarifying much of the controversy surrounding high-field transport in III-V nitrides, including the effect of nonequilibrium hot-phonons on carrier dynamics.

The authors gratefully acknowledge financial support from the Office of Naval Research (Dr. C. Wood), and the University of Notre Dame research funds.

[1]B. K. Ridley, W. J. Schaff, and L. F. Eastman, J. Appl. Phys. **96**, 1499 (2004).
[2]M. Ramonas, A. Matulionis, J. Liberis, L. F. Eastman, X. Chen, and Y.-J. Sun, Phys. Rev. B **71**, 075324, (2005).
[3]K. T. Tsen, D. K. Ferry, A. Botchkarev, B. Sverdlov, A. Salvador, and H. Morkoc, Appl. Phys. Lett. **72**, 2132 (1998).
[4]A. Matulionis (unpublished).
[5]F. Bernardini, V. Fiorentini, and D. Vanderbilt, Phys. Rev. B **56**, R10 024 (1997).
[6]D. Jena, S. Heikman, D. Green, D. Buttari, R. Coffie, H. Xing, S. Keller, S. DenBaars, J. Speck, U. K. Mishra, and I. P. Smorchkova, Appl. Phys. Lett. **81**, 4395 (2002).
[7]S. Rajan, H. Xing, S. DenBaars, U. K. Mishra, and D. Jena, Appl. Phys. Lett. **84**, 1591 (2004).
[8]H. Kroemer, W. Y. Chien, J. S. Harris, Jr., and D. D. Edwall, Appl. Phys. Lett. **36**, 295 (1980).
[9]J. H. Davies, *The Physics of Low-Dimensional Semiconductors*, 1st ed. (Cambridge University Press, Cambridge, UK, (1998).
[10]J. L. Smith and P. J. Stiles, Phys. Rev. Lett. **29**, 102 (1972).
[11]K. Seeger, *Semiconductor Physics, An Introduction*, 6th ed. (Springer, Berlin, 1999).
[12]D. C. Look and R. J. Molnar, Appl. Phys. Lett. **70**, 3377, (1997).
[13]D. Jena, A. C. Gossard, and U. K. Mishra, Appl. Phys. Lett. **76**, 1707 (2000).
[14]N. G. Weimann, L. F. Eastman, D. Doppalapudi, H. M. Ng, and T. D. Moustakas, J. Appl. Phys. **83**, 3656 (1998).
[15]C. Hamaguchi, *Basic Semiconductor Physics* (2001), p. 280.
[16]W. B. Joyce and R. W. Dixon, Appl. Phys. Lett. **31**, 354 (1977).
[17]L. Hsu and W. Walukiewicz, J. Appl. Phys. **89**, 1783 (2001).
[18]M. A. Khan, J. N. Kuznia, D. T. Olson, T. George, and W. T. Pike, Appl. Phys. Lett. **63**, 3470 (1993).